

ERDC/CRREL MP-20-10

Cold Regions Research and
Engineering Laboratory



**US Army Corps
of Engineers®**
Engineer Research and
Development Center



Street-Scale Mapping of Urban Radio Frequency Noise at Very High Frequency and Ultra High Frequency

Daniel J. Breton, Caitlin E. Haedrich , Matthew J. Kamrath, and
D. Keith Wilson

August 2020

The U.S. Army Engineer Research and Development Center (ERDC) solves the nation's toughest engineering and environmental challenges. ERDC develops innovative solutions in civil and military engineering, geospatial sciences, water resources, and environmental sciences for the Army, the Department of Defense, civilian agencies, and our nation's public good. Find out more at www.erdclibrary.on.worldcat.org/discovery.

To search for other technical reports published by ERDC, visit the ERDC online library at <http://www.erdclibrary.on.worldcat.org/discovery>.

Street-Scale Mapping of Urban Radio Frequency Noise at Very High Frequency and Ultra High Frequency

Daniel J. Breton, Caitlin E. Haedrich , Matthew J. Kamrath, and D. Keith Wilson

*Cold Regions Research and Engineering Laboratory
U.S. Army Engineer Research and Development Center
72 Lyme Road
Hanover, NH 03712*

Final report

Approved for public release; distribution is unlimited.

Prepared for U.S. Army Corps of Engineers
Washington, DC 20314

Under Program Element 0611102T, Project Number T442, and Task Number 01

Preface

This study was conducted for the U.S. Army Corps of Engineers under Program Element 0611102T, Project T442, and Task Number 01. The Technical monitor was Dr. Marino A. Niccolai.

The work was performed by the Signature Physics Branch of the Research and Engineering Division, U.S. Army Engineer Research and Development Center, Cold Regions Research and Engineering Laboratory (ERDC-CRREL). At the time of publication of this Miscellaneous Paper, Mr. Dr. Marino A. Niccolai was Branch Chief; Mr. James Horne was Division Chief; and Dr. Robert Davis was the Technical Director for Geospatial Research and Engineering. The Deputy Director of ERDC-CRREL was Mr. David B. Ringelberg, and the Director was Dr. Joseph L. Corriveau.

This Miscellaneous Paper (MP) was originally published online 8 October 2019 as the following: Breton, Daniel J., Caitlin E. Haedrich, Matthew J. Kamrath, and D. Keith Wilson. 2019. "Street-Scale Mapping of Urban Radio Frequency Noise at Very High Frequency and Ultra High Frequency." *Radio Science* 54 (11): 934–48.

<https://doi.org/10.1029/2019RS006893>. This work was funded by the Assistant Secretary of the U.S. Army (Acquisition, Signature Physics and Terrain State Basic Research & Mapping and Remote Sensing) with portions funded under 611102T2400/T442/T24 and 61110252C00/T360/52C/01.

The Commander of ERDC was COL Teresa A. Schlosser and the Director was Dr. David W. Pittman.

Street-Scale Mapping of Urban Radio Frequency Noise at Very High Frequency and Ultra High Frequency

Abstract Modern measurement campaigns of man-made radio frequency (RF) noise have reported results from fixed locations that are assumed to be representative of the surroundings. Models derived from these measurements include parameters to express the variability in time and in space over very large distances (i.e., differences between cities). Despite the rapidly evolving mixture of noise sources, especially in modern urban environments, spatial variation of RF noise power at the scale of streets and blocks is essentially unknown in the very high frequency and ultra high frequency bands. Using a portable calibrated noise measurement system of our design, RF noise was recorded over a 1-MHz bandwidth for frequencies of 142.0, 246.5, and 972 MHz. Noise surveys were conducted during daytime working hours in two different neighborhoods within Boston, Massachusetts, USA, with each survey transiting a fixed, several kilometer long route, repeated twice to enable separation of temporal from spatial variability. Significant and spatially repeatable variations in median power, peak power, and voltage deviation were observed over distances of tens to hundreds of meters, dependent upon the measurement frequency. The observed spatial patterns of median and peak power appear to be repeatable on timescales of hours to weeks, and likely beyond, suggesting that these noise patterns are persistent features of the urban environment.

1. Introduction

Published studies of urban-related radio frequency (RF) noise date back to at least the 1940s (George, 1940), with significant efforts from 1960 to 1970 (Buehler & Lunden, 1966; Bruckert & Sangster, 1969; Skomal, 1965; 1970) and continuing to the present day (Fockens et al., 2019; Middleton, 1973; Palaios et al., 2018; Parsons & Sheikh, 1981; Skomal, 1978). Nearly all of these measurements were conducted from a small number of fixed locations (Achatz & Dalke, 2001; Dalke et al., 1997; Esposito & Buck, 1973; Wagstaff & Merricks, 2005; Wepman & Sanders, 2011) using large vehicles to house the necessary equipment, power supplies, and temperature control and provide suitable mounting structures for the measurement antenna. These fixed measurement locations were chosen to be representative of generic classes of urbanization generally labeled *quiet rural*, *rural*, *residential*, and *city*, listed in order of increasing expected noise power.

Few exceptions in the literature to the “fixed site” measurement concept can be found. The work of Spaulding et al. (1971), and Spaulding and Disney (1974), as well as a series of airborne measurements over major urban areas (Cudak et al., 1991; Ploussios, 1968; Skomal, 1969; 1975; Roy, 1981) appear to be the only exceptions. The airborne measurements indicated that noise power was smooth (on the several kilometer scale, when measured at sufficient altitude) and approximately symmetrical about the centroid of the overflowed urban area and that intentional emissions from urban areas were detectable at distances of a few hundred kilometers (again, dependent upon altitude) for airborne measurements.

The mobile noise campaign of Spaulding et al. (1971) conducted within various neighborhoods of San Antonio, Texas, in 1968, is particularly relevant to the work presented in this paper because they conducted ground-level measurements of urban noise *in motion* and on the scale of *individual streets*. Their measurement system sampled noise at several frequencies below 50 MHz, and though the measurements were collected on a 10-s interval while traveling at vehicular speeds, the resulting noise profiles still show significant variations in noise power over spatial scales of city blocks (15 dB rel. $k_B T_0$ over distances of 160 m at 48 MHz), where k_B is Boltzmann’s constant and T_0 is 290 K.

While the work of Spaulding et al. (1971) represents the first true few wavelength scale “maps” of RF noise in urban environments, their work statistically characterized entire neighborhoods (Spaulding & Disney, 1974) and sought to establish connections with vehicular traffic density, rather than investigating questions

regarding the spatial and temporal persistence of the urban noise field. Repeat measurement laps were reported in the text, but there were no plots or analyses of these repeat laps to separate persistent *spatial fluctuations* from *temporal transients* in noise power over time, and only profiles of median power were created from these data.

Military and first-responder organizations commonly use the very high frequency (VHF) and ultra high frequency (UHF) bands for ground-to-ground communications. For these users, predictions of RF noise levels on spatial scales encompassing entire cities do not provide understanding of the magnitude or spatial scale of noise power fluctuations in the urban environment. Awareness of the street-scale structure of urban RF noise could help in planning events and devising mitigation strategies when operating in urban terrain. The overall goal of this paper then is to provide a preliminary answer to the question, “Do modern RF noise fields in the VHF and UHF bands vary at street scales, and are their statistical characteristics persistent over time and space?”

Our results suggest that the spatial patterns of urban noise (viewed with three summarizing statistics: median power, peak power, and voltage deviation) are persistent features of the urban environment on time-scales of hours to weeks and possibly longer. We conclude that urban noise in the VHF and UHF bands can (and perhaps should) be mapped on the street scale, as such maps could be used to improve the reliability of ground-to-ground communications and to identify particularly offensive RF noise clusters within the urban environment.

2. Methods

In order to answer the question posed in section 1, we developed a portable RF noise measurement system suitable for use in dense urban terrain and then conducted noise surveys within two different neighborhoods of Boston: Downtown and the North End.

2.1. Portable Noise Measurement System

Conducting mobile measurements necessarily involves compromises between weight, power consumption, dynamic range, antenna size, temperature and mechanical stability, and self-noise of the measurement and transportation systems used. To eliminate (self-)vehicular noise, we designed a highly portable measurement system capable of being carried on a frame backpack. This design is also consistent with our desire to characterize urban noise in locations accessible by soldiers and first responders.

Details and photographs of our measurement system can be found in Haedrich and Breton (2019), so only an overview and key performance characteristics are presented here. We used a calibrated, broadband biconical antenna (SAS-545, A.H. Systems, Chatsworth, CA) for all measurements, fed to a tunable 1% band-pass preselection filter (BT-series, K&L Microwave, Salisbury, MD) via a 2.5-m LMR-400 coaxial cable. The band-pass-filtered signal is fed to a low-noise preamplifier (PAM-0202, A.H. Systems), powered by a small 12-V sealed lead-acid battery. An in-line limiter (VLM-63-2W+, Mini-Circuits, Brooklyn, NY) follows the preamplifier and protects the real-time spectrum analyzer from overload.

Recording of in-phase and quadrature (I and Q) data was performed on a real-time spectrum analyzer (BB60C, Signal Hound, Battle Ground, WA) connected to and powered by a Getac B300 ruggedized laptop equipped with a solid-state drive to ensure sufficient data recording throughput, as shown in Figure 1. Our entire system weighed 15.4 kg, including the backpack frame, fiberglass antenna mast, and cabling.

The BB60C operated in zero-span mode at a 1.25-MSample/s sampling rate and an effective recording bandwidth of 1 MHz. The recording bandwidth is chosen within the BB60C’s “Spike” control software (SignalHound, 2019) by a digital Blackman-windowed sinc filter acting on the I and Q data stream. Both the RF recorder and laptop computer were housed inside of an aluminum briefcase, modified with standard bulkhead connectors, to shield the measurement antenna from the significant RF noise produced by the laptop. The system was able to operate for 4 hr before battery replacement was necessary, enabling several kilometers of surveys to be completed on a single laptop battery.

The entire RF recording system, minus the antenna, was calibrated using the Y-factor method (Keysight, 2018) and a calibrated diode noise source (Model NW6G-15-CS, Noisewave, Whippany, NJ). While the overall noise figure of our system (see Table 1) is comparable with earlier works (Achatz &

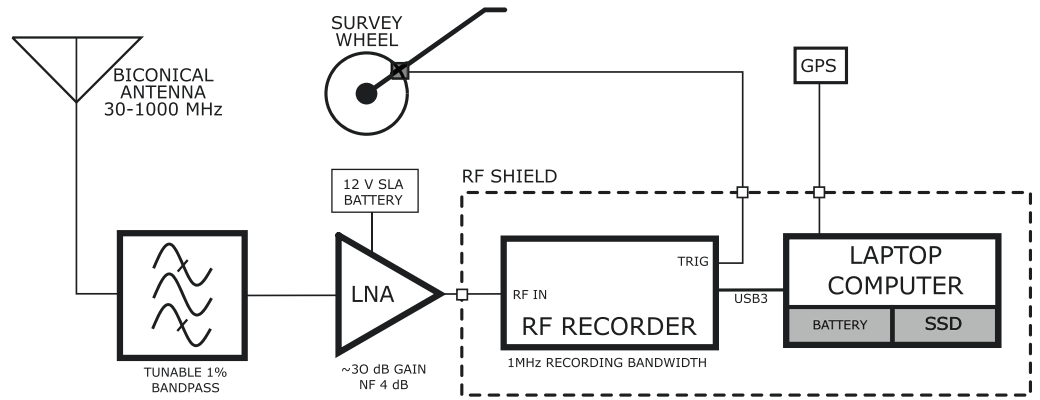


Figure 1. Block diagram of the portable noise measurement system. LNA = low-noise amplifier; RF = radio frequency; SSD = solid-state drive.

Dalke, 2001; Wepman & Sanders, 2011), the dynamic range of our system (45 to 50 dB) is limited compared to the heavier, larger, more energy intensive, and more expensive laboratory-grade instruments used in those studies (69 dB or more). The main trade-off for portability and low-power consumption is therefore dynamic range, limiting our ability (in only a handful of samples at 142 MHz in Downtown Boston) to fully capture the peak power of impulsive events.

2.2. Measurement Positioning

An early version of the system used a small USB-based GPS device, also logged on the laptop, to locate each measurement in space. While this method can work in rural and suburban areas, we (and others, see Paulson, 2019) have found that the attenuation and multipath associated with urban canyons led to unacceptable performance: many tens of meters of positioning error or long sections of data without position were common. We therefore developed a simple and inexpensive positioning method for deep urban work utilizing predetermined routes and tracking our distance along those routes through the use of a survey wheel. We modified a standard survey wheel (Model RT-312M, Rolatape, Watseka, IL) to send a 3.7-V trigger signal to the BB60C for every full revolution (1 m/rev) in order to locate our measurements in space. When triggered, the BB60C captured a 250-ms recording to the solid-state drive on the laptop, resulting in one ~1.2-MB data file per meter.

2.3. Field Measurement Procedure

Prior to commencing field measurements, we conducted several hours of stationary RF spectrum surveys, seeking unoccupied regions of sufficient bandwidth. Our search led us to choose 142.0, 246.5, and 972.0 MHz as the center frequencies of our measurement bands, each of which lies within a U.S. federal-exclusive portion of the spectrum. Spectral and statistical examination of our data in postprocessing shows that no narrowband emitters were recorded with the exception of a handful of measurements at 972.0 MHz.

Mapping measurements were performed during normal working hours on weekdays, along predetermined routes roughly 2 km in length. Approximately 1 hr was required to traverse a route on foot, one time. The distance traveled between route control points (corners, intersections, etc.) was noted from the survey wheel

Table 1
Overall Noise Measurement System Characteristics for 1-MHz Effective Noise Bandwidth

Frequency (MHz)	Noise figure (dB)	Overall gain (dB)	Minimum detectable power (dBm)	Maximum detectable power (dBm)	Antenna gain (dBi)
142.0	7.6	17.8	-106.5	-52.3	-9.3
246.5	6.6	30.7	-107.4	-65.2	+2.7
972.0	5.2	30.6	-108.9	-64.9	+1.4

Note. Overall gain includes antenna gain, while minimum and maximum detectable power do not.

in the field, and the resulting data were located through linear interpolation in postprocessing. Measurement along the paths were repeated two times in succession to enable detection and separation of transient from spatially persistent noise features. The routes were typically traversed by a team of two: one person to carry the backpack system and operate the survey wheel and another to carry spare batteries, take notes on distance and location, and to start/stop recordings on the laptop.

3. Results

The data presented in this paper were primarily recorded on 9–10 October 2018 in the Downtown and North End neighborhoods of Boston, with additional collection of 142.0-MHz measurements Downtown on 24 October 2018. We present our results, by neighborhood, in three main formats.

1. Maps showing the spatial relationships between various noise characteristics and the urban environment itself. Maps for median and peak powers not shown here can be found in the Supporting Information.
2. Histograms of noise characteristics drawn from entire neighborhoods to show the distribution of measured noise levels over space.
3. Plots of noise characteristics versus distance to show repeatability between laps and persistence in both time and space.

We use three summarizing noise statistics to describe our results as functions of frequency and space: median power, peak power (defined as the power threshold for the upper 0.01% of the distribution; Achatz, 1998; Wepman & Sanders, 2011), and voltage deviation. After briefly reviewing voltage deviation, we describe the overall results for both of our study neighborhoods and then discuss and analyze the spatial repeatability.

Voltage deviation (Crichlow et al., 1959, 1960; Skomal & Smith, 1985; Spaulding et al., 1971; Spaulding & Disney, 1974) is defined as

$$V_d = 20\log_{10}\left(\frac{V_{\text{rms}}}{V_{\text{mean}}}\right), \quad (1)$$

where V_{rms} and V_{mean} are the root-mean-square and mean, respectively, of the measured noise voltage envelope. The voltage deviation is an older but straightforward metric for the impulsive character of noise, free from assumptions regarding the underlying statistical distribution of the noise itself, or subjective assessments of slope changes on amplitude probability distribution plots (Wagstaff & Merricks, 2005). These qualities make it especially appealing for mapping, as it provides a single, easily interpreted value describing the impulsive character of the local noise field. A circular complex Gaussian noise source (i.e., one with a Rayleigh-distributed amplitude and exponentially distributed power, also sometimes called “thermal” or “thermalized” in the literature) will approach a value of $V_d=1.05$ dB. The presence of an interfering narrowband signal in the recording results in $V_d<1.05$ dB, while the presence of impulsive noise yields $V_d>1.05$ dB.

3.1. Downtown Boston

The 2.14-km route through Downtown, shown in Figure 2, was chosen to sample both deep urban core areas and more open areas along the Greenway. Downtown is surrounded on all sides by other neighborhoods with the exception of the Atlantic Ocean directly to the east. The largest spatial variations in median and peak power, and the largest values of voltage deviation, were observed in deep urban canyons. The smallest variations in all three statistics occurred in the open areas along the Greenway, covering distances 900–1,500 m on Figure 3. Spatial variations in all statistics decreased with increasing frequency, as shown in Table 2 and Figure 3.

Data collected on repeat laps showed remarkable repeatability (discussed in more detail below) and evidence of only small temporal fluctuations between laps (i.e., on the hour timescale). Such a fluctuation at 142 MHz can be perceived in the roughly 5-dB difference in median power between Laps 1 and 2 near the eastern corner of the route in Figure 2, located around the 1,400 m point of Figure 3. Large differences in peak power and voltage deviation are also observed for this location, suggesting that impulsive noise present on Lap 1, but not present on Lap 2, is the cause for the discrepancy in median powers in this case.

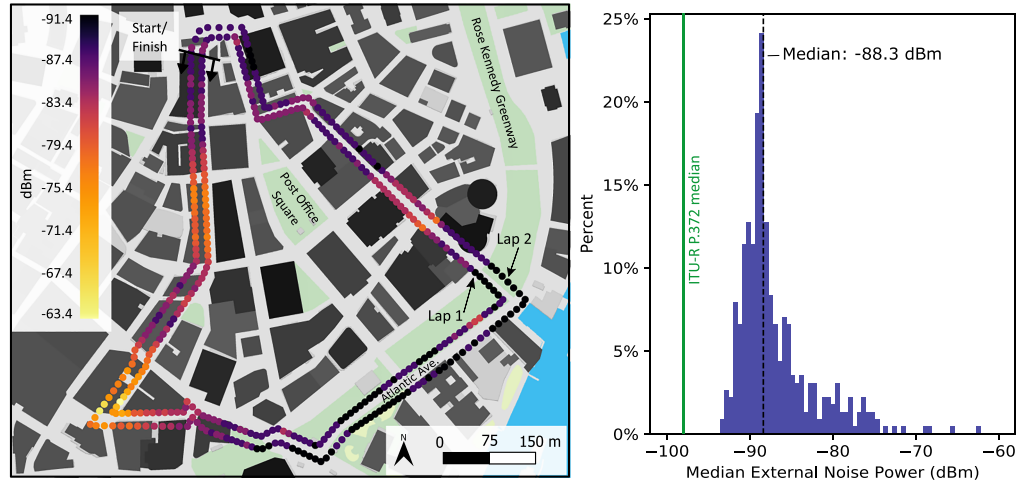


Figure 2. Map and histogram of median external noise power for 1-MHz measurement bandwidth in Downtown Boston at 142.0 MHz. While measurements were taken every meter, points on the maps are calculated from 10-m segments of spatially adjacent data to improve clarity. Darker shaded buildings are taller than lighter ones. Inner lap points (Lap 1) show the true location of the measurements, while the outer lap (Lap 2) points have been displaced outward by affine transformation to allow side-by-side comparison of two repeat laps on one map. ITU-R P.372-13 predicted F_{am} for the “city” environmental category is shown on the histogram for comparison.

In terms of data quality for the Downtown neighborhood, we note that (1) system dynamic range limitations prevented us from fully capturing peak power at 142 MHz in the vicinity of 600 m, and (2) a short section of data for 972 MHz, Lap 1, appears to be compromised by a narrowband emission just before the 500-m mark, as shown by voltage deviation <1.05 dB. The remainder is free of intentional emitters and within the system dynamic range, as shown in Figure 3.

3.2. North End

The 2.32-km route through the North End was chosen to include major thoroughfares along the western edge of the neighborhood, as well as the retail zone along Hanover Street and quiet residential streets. This neighborhood is bound on the west and south by Downtown Boston and on the north and east by water; Logan International Airport is 3 km to the northeast.

Overall, the North End contained lower median and peak powers and generally higher voltage deviation values compared to Downtown. Like Downtown, spatial variations in all three summarizing statistics decreased with increasing frequency in the North End, as shown in Table 2 and Figure 5. Several noise clusters are apparent along the western edge of the neighborhood, along the heavily retail Hanover Street, and in the vicinity of the U.S. Coast Guard station on Commercial St, as shown in Figure 4.

Similar to Downtown, the repeat lap data for median power from the North End showed excellent spatial repeatability. Peak power for 142 and 246.5 MHz was also reasonably repeatable; however, some significant differences in peak power occurred between laps at 972 MHz around 1,600 and 2,000 m. On Lap 2, V_d was high and remained above the thermal limit and, together with high peak power in these sections, suggest the presence of strong impulsive broadband noise on Lap 2 that was not present on Lap 1. Measured median power at 972 MHz is often very close to the minimum system sensitivity in the North End, and thus, statistics derived from these data are not reported (Figure 4).

3.3. Repeatability

We have chosen three metrics, based on the work of Bland and Altman (1987), to quantify lap-to-lap repeatability in our data: the mean absolute difference (MAD), the root-mean-square difference (RMSD), and the normalized mean absolute difference (NMAD), all calculated by comparing measurements on a position-by-position basis. Let the vectors $\mathbf{x}=\{x_1,\dots,x_N\}$ and $\mathbf{y}=\{y_1,\dots,y_N\}$ represent the N measurements of a given quantity on different repeat laps. x_i and y_i then represent measurements at a shared position i . Defining our metrics on a position-by-position basis, we have

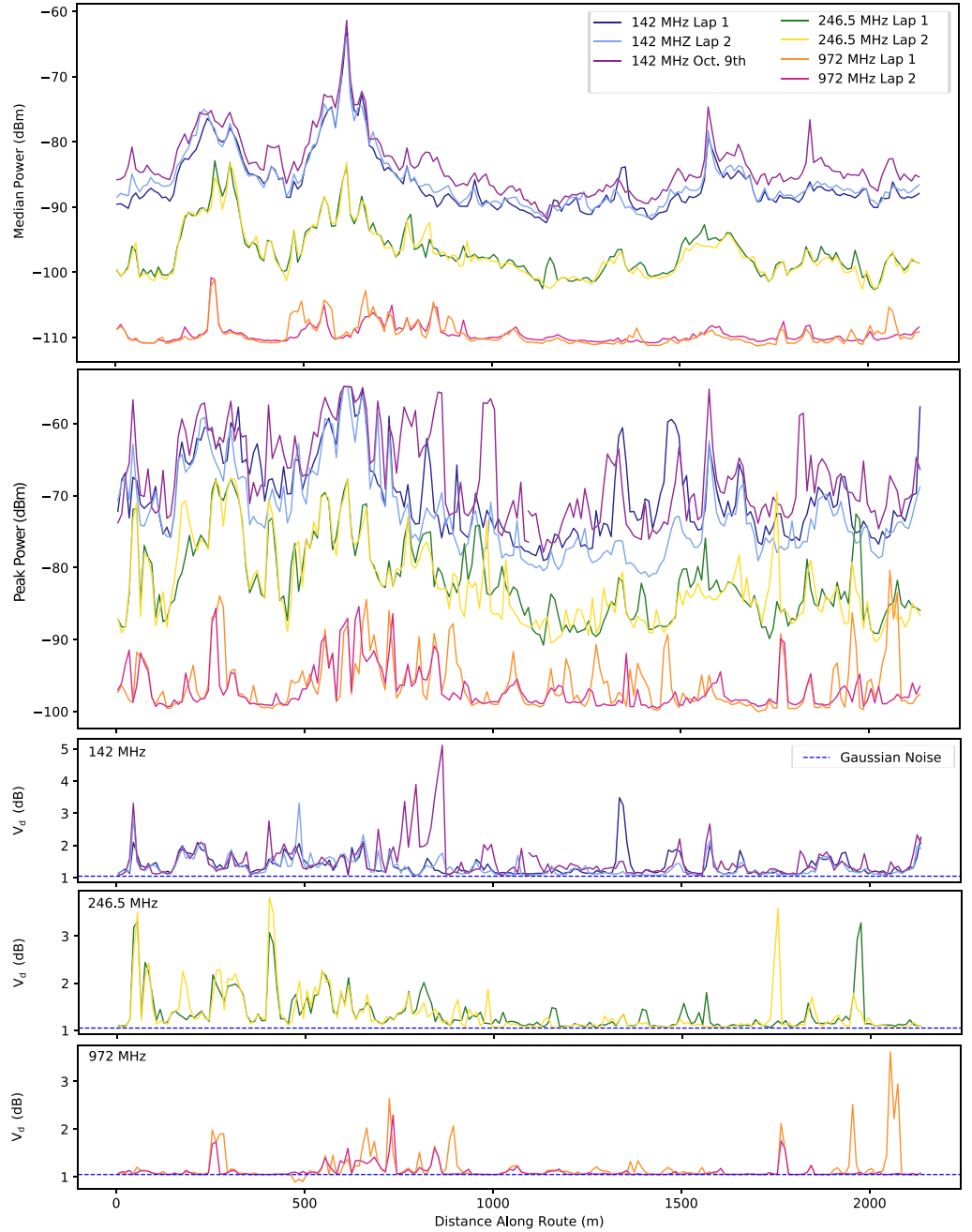


Figure 3. Plot of the summarizing statistics as a function of distance along route in Downtown Boston. Laps 1 and 2 for 142 MHz conducted 24 October. The limiting value of voltage deviation for thermal noise shown as dashed line.

$$\text{MAD}(\mathbf{x}, \mathbf{y}) = \frac{1}{N} \sum_{i=1}^N |x_i - y_i| \quad (2)$$

and

$$\text{RMSD}(\mathbf{x}, \mathbf{y}) = \sqrt{\frac{1}{N} \sum_{i=1}^N (x_i - y_i)^2}. \quad (3)$$

With the exception of the $1/N$ normalizing factors (included because DT and NE data sets are not of the same length), MAD and RMSD are equivalent to the L1 and L2 distance functions, or “norms,” commonly used to

Table 2

Measurement Statistics for all Measurements Collected at a Given Frequency, in a Given Neighborhood, for a 1-MHz Bandwidth

Neighborhood	Frequency (MHz)	Minimum (dBm)	Maximum (dBm)	Range (dB)	Median (dBm)	SD (dB)
Downtown	142.0	-93.8	-60.6	33.2	-88.3	4.7
North End	142.0	-98.8	-69.3	29.5	-93.7	3.4
Downtown	246.5	-103.4	-77.4	26.0	-97.9	4.0
North End	246.5	-108.7	-84.4	24.3	-102.8	3.4

Note. Data at 972 MHz are at or near the minimum system sensitivity for both neighborhoods; therefore, we do not report overall statistics for this frequency.

assess time series similarity (Morse & Patel, 2007). The MAD and RMSD metrics are calculated using decibel values for the \mathbf{x} and \mathbf{y} , to give a general sense for the magnitude of lap-to-lap differences and variability. The NMAD is defined as

$$\text{NMAD}(\mathbf{x}, \mathbf{y}) = \frac{\frac{1}{N} \sum_{i=1}^N |x_i - y_i|}{\max(x_{\max}, y_{\max}) - \min(x_{\min}, y_{\min})}, \quad (4)$$

where $x_{\max} = \max(x_i)$, $x_{\min} = \min(x_i)$, and so on. Because of the quotient in the NMAD expression, it is necessary to use linear values (expressed in mW) for \mathbf{x} and \mathbf{y} in order to evaluate it correctly.

The MAD value represents the expected typical difference (in dB) between measurements x_i and y_i at a randomly chosen location i . Smaller MAD values indicate better spatial repeatability. Likewise, RMSD values represent the expected variation (in dB) in the difference between co-located measurements at a randomly chosen i . If the lap-to-lap differences can be assumed to be normally distributed (an assumption generally supported by the data), then roughly 68% of the lap-to-lap differences should be contained within a range of one RMSD about the mean difference, $(1/N) \sum (x_i - y_i)$. The NMAD describes the size of expected lap-to-lap differences relative to the range of observations encountered along an entire route, providing a figure for comparing the relative repeatability between the different measurements of median power, peak power, and voltage deviation.

As shown in Table 3, both MAD and RMSD for median noise power decrease with frequency, suggesting that higher frequency measurements of median power are generally more repeatable. While median power MAD

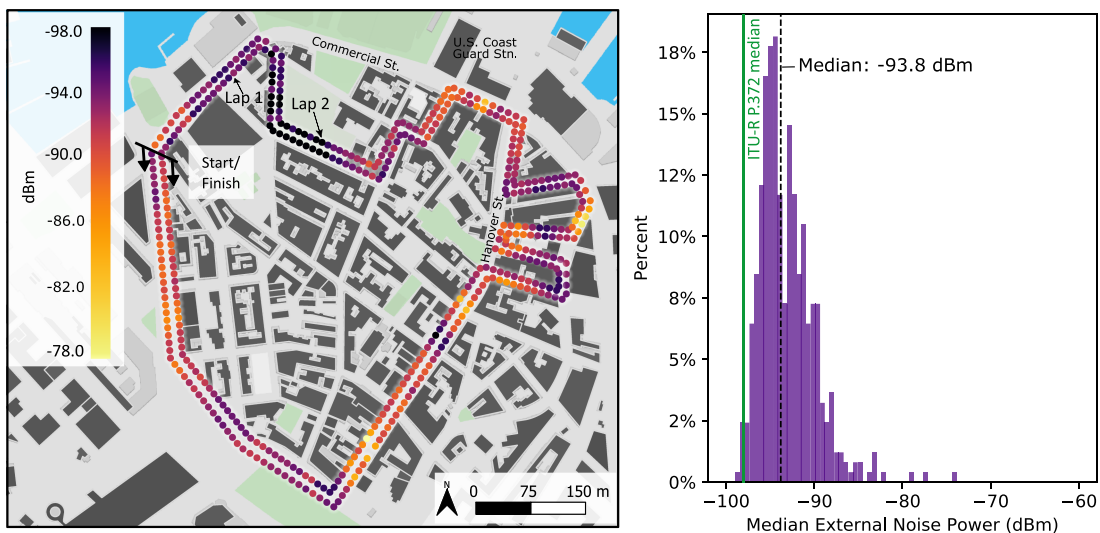


Figure 4. Map and histogram of median external noise power for 1-MHz measurement bandwidth in North End at 142.0 MHz. As before, inner lap points (Lap 1) show the true location of the measurements. ITU-R P.372-13 predicted F_{am} for the “city” environmental category is shown for comparison.

Table 3
Repeatability Statistics (MAD and RMSD Expressed in dB) for Two Same-Day Repeat Laps Collected in a Given Neighborhood (DT = Downtown; NE = North End) at a Given Frequency (MHz)

Location	Frequency	Median power			Peak power			Voltage deviation		
		MAD	RMSD	NMAD	MAD	RMSD	NMAD	MAD	RMSD	NMAD
DT	142.0	1.26	1.59	0.50%	3.14	4.52	3.85%	0.15	0.30	5.35%
NE	142.0	1.42	1.95	0.98%	3.68	5.39	3.66%	0.11	0.80	5.36%
DT	246.5	0.72	1.07	1.35%	2.02	3.20	3.56%	0.15	0.32	4.61%
NE	246.5	0.82	1.33	1.18%	3.59	5.70	5.62%	0.37	0.89	3.04%

Note. Because data recorded for 972 MHz is often close to or at the instrument noise floor, we do not analyze it here. MAD = mean absolute difference; NMAD = normalized mean absolute difference; RMSD = root-mean-square difference.

values decreased with frequency, the overall range of observations decreased to a greater extent, leading to increases in NMAD with frequency. Peak power and voltage deviation show no apparent frequency dependence and were not as repeatable as median power as indicated by the larger MAD, RMSD, and NMAD values. NMAD values for all of the summarizing statistics are under 6%, indicating that a typical lap-to-lap difference is small relative to the overall range of positional differences in the data. Because it is normalized, the NMAD also provides a way to objectively compare the relative spatial repeatability of different data sets: Overall, median power is more repeatable than peak power, which is (usually) more repeatable than voltage deviation. This ordering of relative repeatability matches our intuition, recognizing the strong influence of impulsive noise on the latter two statistics.

In order to assess spatial repeatability over a longer timescale, Table 4 compares two repeat laps of 142-MHz data collected on 24 October 2018 to a single lap of data collected over 2 weeks earlier on 9 October in Downtown Boston. These results show that even over multiple weeks, the spatial pattern of median noise power is generally repeatable to within a few decibels. Peak power and voltage deviation are generally less repeatable over this timescale, but several distinct noise clusters (located at approximately 60, 250, 600, 1,550, and 1,700 m in Figure 3) are visible in all three sets of data.

4. Discussion

There are several features of the data from both neighborhoods that are worth discussing, including

1. a comparison of observed median noise powers, and upper and lower decile deviations based on neighborhood-scale spatial measurements, with those reported in the literature,
2. the characteristic length of noise clusters observed in our study neighborhoods,
3. the repeatability and temporal persistence of spatial patterns for a given statistic, and the spatial relationship between statistics, and
4. the observed relationship between urban morphology and impulsive noise content.

4.1. Comparison with Other Published Measurements

Overall, our measurements in the Boston area have higher median powers and more variability at a given frequency than previous work. Our primary comparisons are with models and reported measurement values

Table 4
Repeatability Statistics (MAD and RMSD Expressed in dB) at 142 MHz for Laps Collected 16 days Apart in Downtown Boston

Lap	Median power			Peak power			Voltage deviation		
	MAD	RMSD	NMAD	MAD	RMSD	NMAD	MAD	RMSD	NMAD
A, B	1.26	1.59	0.50%	3.14	4.52	3.85%	0.15	0.30	5.35%
A, C	3.59	4.09	0.99%	5.48	6.37	8.53%	0.64	1.01	7.67%
B, C	2.70	3.36	0.57%	4.06	5.15	8.00%	0.66	1.04	7.96%

Note. A = Lap 1 on 24 October; B = Lap 2 on 24 October; C = Lap on 9 October; MAD = mean absolute difference; NMAD = normalized mean absolute difference; RMSD = root-mean-square difference.

Table 5
Comparison of Median External Noise Power, Expressed in Decibels Relative to $k_B T_0 b$ for a $b=1$ -MHz Equivalent Noise Bandwidth, for Relevant Earlier Studies and Models

Frequency (MHz)	DT Boston	NE Boston	WS	AD	ITU-T4	ITU City	ITU Residential
112.5	—	—	28.1	—	—	20.0	15.7
121.0	—	—	—	—	15.5	19.1	14.8
137.5	—	—	—	17.6	—	17.6	13.3
142.0	25.7	20.3	—	—	—	17.2	12.9
163.0	—	—	—	—	13.0	15.5	11.2
221.5	—	—	14.9	—	—	11.8	7.5
222.0	—	—	—	—	9.0	11.8	7.5
246.5	16.1	11.2	—	—	—	10.5	6.2

Note. Values for Boston Downtown (DT) and North End (NE) are neighborhood-wide spatial medians, while Wepman and Sanders (2011; WS), Achatz and Dalke (2001; AD), and ITU-R P.372-13 Table 4 “Outdoor man-made noise measurements in Japan” (ITU-T4) are temporal medians for fixed locations. Modeled values are from equation 13 of ITU-R P.372-13.

listed in ITU-R P.372-13 (hereafter simply “ITU”), though other references are included where appropriate. Direct comparison with other references is generally difficult; the duration of measurements, frequencies, bandwidths, antennae, locations, and methodologies vary from study to study. Table 5 compares our F_{am} results with two similar studies conducted in the United States, Wepman and Sanders (2011) and Achatz (1998), while Table 6 compares variability, expressed as decile deviations, between our work, ITU, and that of Spaulding et al. (1971) where spatial variability on the neighborhood scale is reported.

Comparing our Downtown and North End values of F_{am} to the ITU City and Residential models, respectively, our results are consistently 5 to 8 dB higher. Similarly, results from Wepman and Sanders (2011) are also significantly higher than the ITU model. The work of Achatz and Dalke (2001) at 137.5 MHz agrees nicely with the ITU City model; however, these measurements were made a decade before that of Wepman and Sanders (2011).

In all of the above comparisons, it is important to remember that our reported F_{am} values, like those of Spaulding et al. (1971) and Spaulding and Disney (1974), and unlike most other measurements, are based on neighborhood-scale *spatial medians*. Our data in Figure 5 show that a stationary measurement even within a dense region of the North End (around 1,000 m, for example) could produce results with in good agreement with the ITU model. A measurement of median power made just 300 m further along our route would disagree with the same model by over 10 dB. Both sites appear on the map, and to the eye, as equivalent heavily urbanized sites, but in reality, they have significantly different noise character.

Table 6
Decile Deviations (in dB)

Decile deviation	Frequency	ITU-T4	DT	NE	SA
Upper (90th percentile)	48.0	—	—	—	13.1
	121.0	5.1	—	—	—
	142.0	—	8.4	4.4	—
	163.0	6.7	—	—	—
	222.0	5.1	—	—	—
	246.5	—	6.8	4.9	—
Lower (10th percentile)	48.0	—	—	—	8.1
	121.0	3.6	—	—	—
	142.0	—	2.7	2.6	—
	163.0	3.4	—	—	—
	222.0	3.0	—	—	—
	246.5	—	3.0	2.9	—

Note. Decile deviations from Downtown (DT) and the North End (NE) of Boston and in San Antonio (SA) Texas SLA-15 from Spaulding et al. (1971) express neighborhood-scale spatial variability. ITU-T4 = ITU-R P.372-13 Table 4, “City” category.

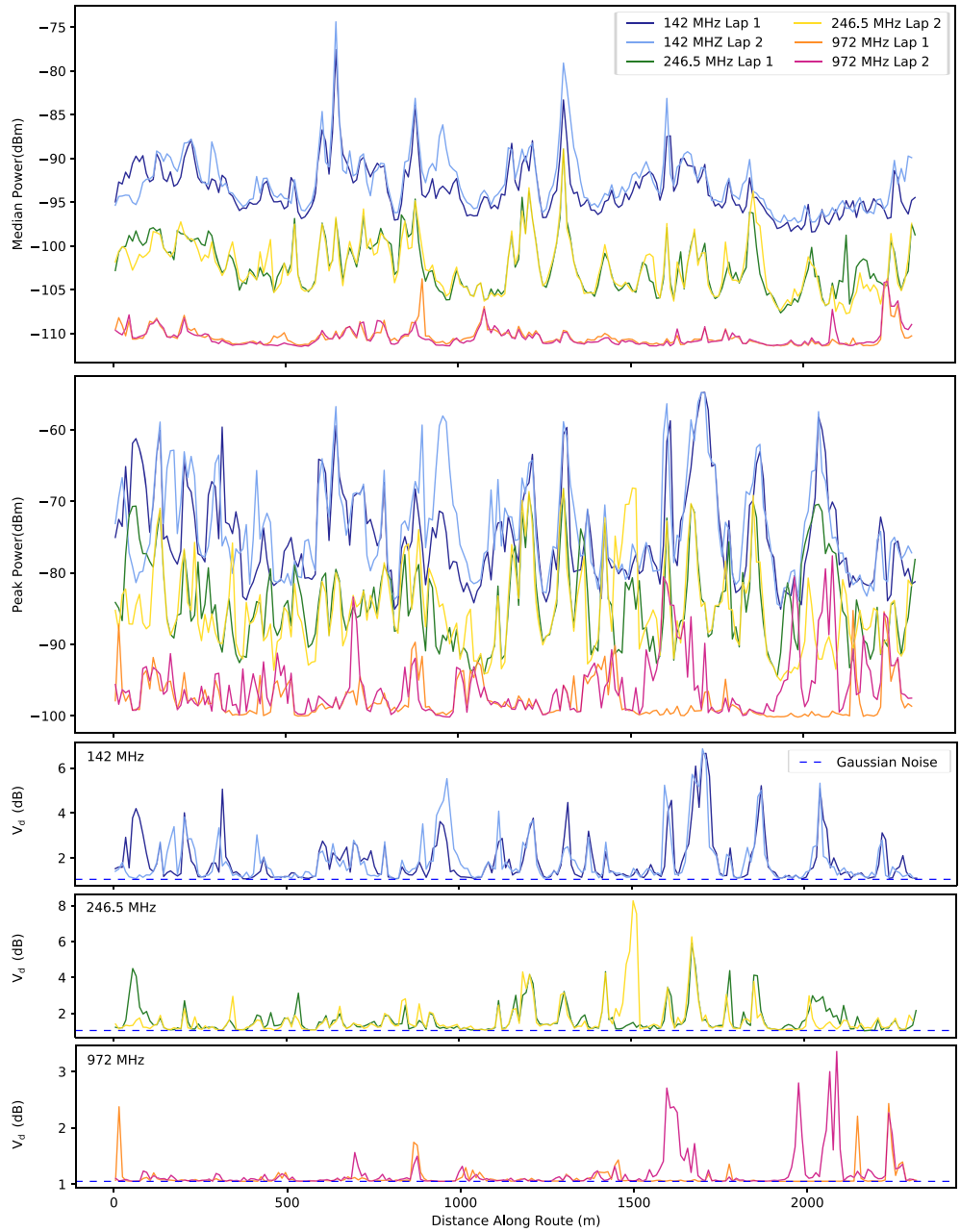


Figure 5. Plot of the summarizing statistics as a function of distance along route in the North End. The minimum system sensitivity at 972 MHz and limiting value of V_d for thermal noise are plotted as dashed lines.

The practice of choosing a single measurement location within subjectively defined environmental categories, without first mapping the RF noise characteristics within that neighborhood, poses risks for mischaracterizing the noise on the neighborhood scale unless many optimally spaced stationary measurements are made. Measurement antennae mounted on tall masts may mitigate some of the spatial variability effect and yield more generalized neighborhood characteristics, but such measurements are likely not representative of the urban RF noise fields actually experienced by ground-based receivers and may be logistically impossible in dense urban areas. Previously reported works have also generally used low antennae: ground level (~ 2.5 m, Leck, 2006; Spaulding & Disney, 1974, this work) or mounted on top of a vehicle (~ 4 m, Achatz & Dalke, 2001; Spaulding et al., 1971; Wagstaff & Merricks, 2005; Wepman & Sanders, 2011). If near-ground measurements are to be the standard for RF noise

measurements, then mapping becomes a critical tool for understanding the larger context of the noise environment surrounding a given set of measurements.

Turning now to a discussion of noise spatial variability, we define the upper and lower decile deviation as the difference between the decibel values of the overall median and the 10th and 90th percentiles of our median noise powers collected over an entire neighborhood (Spaulding et al., 1971). Our decile values therefore represent neighborhood-scale spatial variability in median noise power. Table 2 in ITU-R P.372-13 recommends, for city environments and frequencies between 0.3 and 250 MHz, upper and lower decile deviations of 8.4 dB for noise power between different instances of the same environmental type, but no particular spatial scale is mentioned.

As shown in Table 6, our decile deviations for median power as a function of location within a given neighborhood disagree with the ITU location variation model in that our measured decile deviations are not symmetric about the median value, as assumed in table 2 of ITU-R P.372. Our lower deviation is much closer to the median, while our upper deviation is similar to the ITU recommendation. Similarly, asymmetric behavior is also seen in the data from Japan presented in ITU Table 4, but because the source of this data is not identified, it is unclear whether these values describe temporal or spatial variability.

4.2. Spatial Structure of Intra-neighborhood RF Median Noise Power

As mentioned in section 1, very few studies have reported on the spatial structure and the range of spatial variations in urban RF noise. Here, we employ a method to determine a characteristic noise cluster length using spatial autocorrelation analysis. We define the normalized autocorrelation function (NACF; Davenport & Root, 1987) of the spatial data series \mathbf{x} as

$$\rho_{\mathbf{xx}}(k = m\Delta d) = \frac{1}{N\sigma_{\mathbf{x}}^2} \sum_{i=1}^{N-m} (x_i - \mu_{\mathbf{x}})(x_{i+m} - \mu_{\mathbf{x}}), \quad (5)$$

where $\mu_{\mathbf{x}}$ and $\sigma_{\mathbf{x}}^2$ are the mean and variance of \mathbf{x} , respectively, k is the lag length, Δd is the distance between measurement points in \mathbf{x} , and m is an integer denoting the number of points comprising a given lag length k .

NACFs for median power along each route (i.e., a one-dimensional spatial series of measurements) were calculated for each repeat lap. The results are plotted in Figure 6 and generally show positive correlation for $k < 100$ m, indicating that RF noise clusters have spatial persistence. The Downtown neighborhood features relatively slowly decaying NACFs for lower frequencies in Downtown and more rapidly decaying NACFs for all frequencies in the North End.

Following Lee et al. (1993), we define the characteristic noise cluster length L_c as the value of the lag at which the NACF drops to $1/e = 0.368$. Using this definition, we determined that Downtown characteristic noise cluster lengths are approximately 110, 94, and 27 m, while North End has noise cluster lengths of approximately 40, 28, and 26 m for frequencies of 142, 246.5, and 972 MHz, respectively. It is unclear at this stage whether the different behaviors NACF decay between neighborhoods should be attributed to the very different propagation environments (deep urban canyons vs. few-story, uniform height buildings) or to the spatial distribution of sources within that environment.

4.3. Spatial Pattern Repeatability

Various measures of spatial repeatability were shown in section 3, indicating that all of our summarizing statistics are repeatable, to varying degrees, on the scale of hours to weeks. Figures 3 and 5 also show spatial correlations between median noise power measured at different frequencies, suggesting that typical clusters are noise sources across a wide range of frequencies: If we observe a high median noise power in a location at one frequency, chances are good that it will be high at another frequency at that same location.

Despite the good spatial repeatability of each of our summarizing statistics, it turns out that none of them is a good predictor of the others. Inspection of Figures 3 and 5 for the case of median power and voltage deviation, for example, the lack of correlation, is obvious. However, comparison of the plots for median and peak powers, and theoretical considerations regarding circular complex Gaussian noise, might suggest that these statistics are related. As we discuss below, this turns out not to be true for a well-known reason: man-made RF noise does not always conform to the circular complex Gaussian ideal.

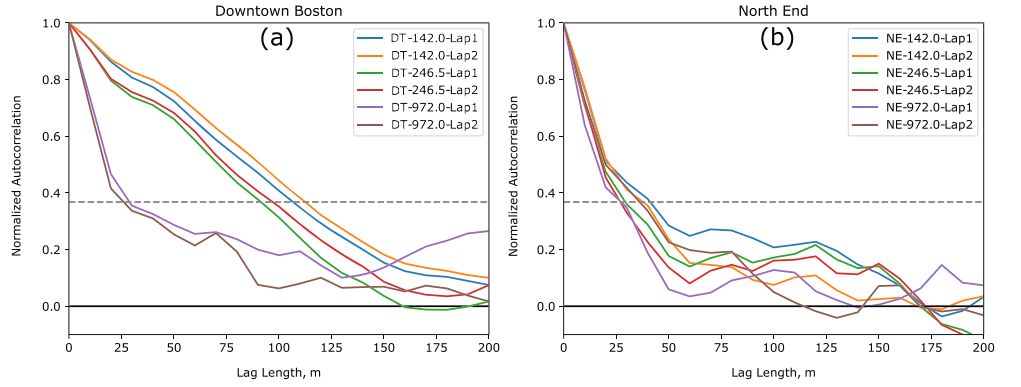


Figure 6. Normalized one-dimensional spatial autocorrelation functions of median external noise power for (a) Downtown Boston and (b) the North End. Dashed line at $1/e$ indicates threshold for determination of characteristic noise cluster length L_c .

Figure 7 plots a two-dimensional histogram of peak power as a function of median power for all of the measurement locations in the North End neighborhood at 142 MHz. If our measurements had captured only ideal thermal-like noise, then all data points would fall along the labeled “thermal” line in Figure 7, and thus, median would be a good predictor of peak power in this case because peak power is directly proportional to median power. The slope of this thermal line depends on one’s definition of peak power and is derived below. For a thermal (circular complex Gaussian) noise source, the probability density function for the signal power s is an exponential distribution

$$f(s|\beta) = \frac{1}{\beta} \exp(-s/\beta), \quad (6)$$

where β is the mean power expressed in watts. For such a distribution, the median power is $\beta \ln(2)$, and quantiles can be expressed as $-\beta \ln(1-p)$ for a given probability p . The ratio R of any given quantile to the median is a constant whose value depends only on the choice of p , given by

$$R(p) = -\frac{\ln(1-p)}{\ln(2)}. \quad (7)$$

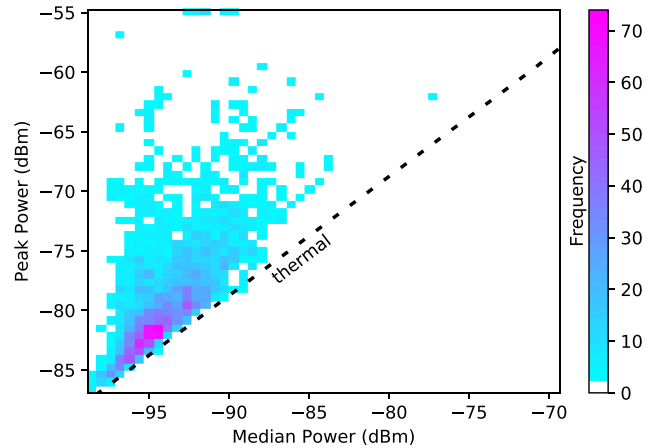


Figure 7. Two-dimensional histogram of peak versus median noise power for the North End at 142 MHz, showing that median power is not a good predictor of peak power. Many measurements are clustered near the overall neighborhood spatial median power (-93.7 dBm) and near the thermal noise line.

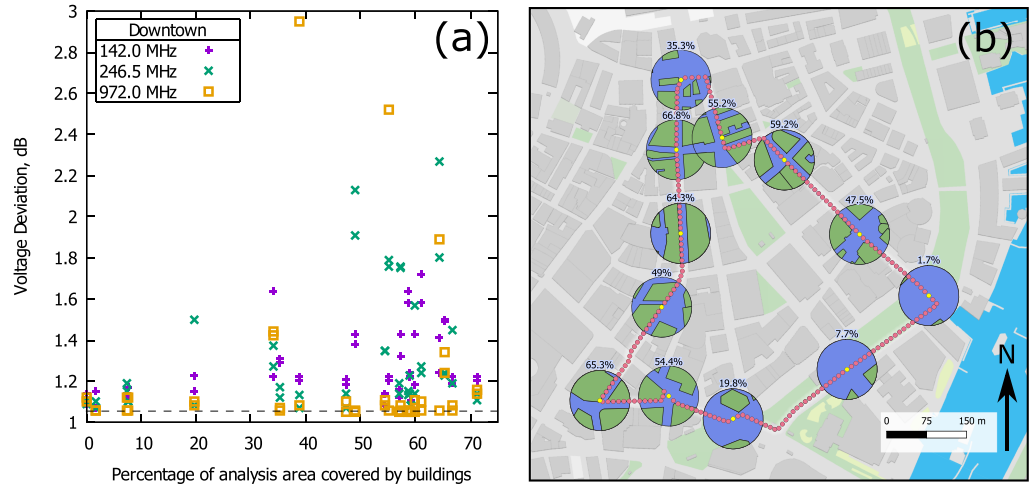


Figure 8. Voltage deviation and urban density in Downtown Boston. (a) V_d versus α at different frequencies. Dashed line is the 1.05-dB thermal limit for V_d . (b) Map of Downtown Boston with analysis circle (radius 56.4 m; area 0.01 km²) centers for α and V_d shown in yellow. Only 12 of the 22 total analysis circles are shown, for clarity.

Following Achatz (1998), Achatz and Dalke (2001), and Wepman and Sanders (2011), if we define the “peak power” threshold at the $p=0.9999$ level, we find $R(0.9999)=13.28$, and thus, the peak power value should theoretically be 11.2 dB greater than median power for a thermal-like noise source. Expressing power in decibel form, a plot of peak versus median power like Figure 7 should therefore result in a straight line along which truly thermal noise sources will fall. Noise measurements contaminated by constant, narrowband emissions would fall below this line, while those containing impulsive noise will lie above it.

All of the points in Figure 7 lie in a wide range above this thermal line, demonstrating that the non-Gaussian nature of man-made noise is the cause for the wide range of peak powers for any given median power. The impulsive component of the noise causes median power to be a poor predictor of peak power and, by extension, V_d . Therefore, while a map of a *given statistic* can, and often does have good repeatability, maps of *different statistics* typically look different from each other. Median and peak power maps can be seen and compared in the Supporting Information.

Given the importance of non-Gaussian characteristics, it is reasonable to ask if the urban environment itself has any influence on the statistical character of urban RF noise. We attempt to address this question in the next section.

4.4. Urban Morphology and Impulsive Content

Plots of median power, peak power, and voltage deviation versus distance shown in Figure 3 suggest a possible relationship between these statistics and the urban morphology of the immediate surroundings, especially as the section from 900 to 1,500 m along the Greenway features low values in all three. Many measures of urban morphology are possible, and in the past, these measures have been used to assess the impact of urban structures on propagation (Kozono & Watanabe, 1977). We use the simplest measure, that of urban areal density α , to understand the impact of urban density on the impulsive character of urban noise. The median and peak noise powers appear to also be influenced by α , but discussion of these statistics and development of models to explain their dependence on α is beyond the scope of this paper.

Following Kozono and Watanabe, we define urban areal density as $\alpha = (\text{building footprint area})/(\text{total analysis area})$ in a 56.4-m radius circle (0.01-km² area) around a given measurement point. This size was chosen to be larger than an average city block (see Figure 8b), and the diameter is also comparable to the characteristic noise cluster lengths in the VHF discussed above. The analysis circles and georeferenced building footprints are “intersected” in GIS software to calculate α around a selected measurement point.

Figure 8a suggests that open areas on the ~0.01-km² scale within a given neighborhood will feature thermalized noise when compared with higher density urban areas. However, the converse is not true: Not all highly

dense urban areas feature strong impulsive components. The variability of voltage deviation appears to increase with urban density, and it may be that this variability is controlled by the spatial density of impulsive sources: Higher urban density implies the *possibility* of higher impulsive noise source densities, whereas more open areas physically cannot contain such sources. Parallels can be drawn with airborne studies of RF noise thermalization as a function of increasing altitude (distance from impulsive sources) over urban centers (Ploussios, 1968; Skomal, 1969, 1978), though naturally, the distances involved are much smaller for ground-based measurements in dense urban environments.

We caution that the above results linking urban morphology to RF noise character are based on a limited spatial sample of a single city center. Similar, though less pronounced, urban density effects are visible in our North End data set. These effects are likely due to the spatial uniformity, the smaller range of urban densities, and to the primarily residential nature of the North End relative to Downtown.

5. Conclusions

The goal of this paper is to answer the question, “Do modern RF noise fields in the VHF and UHF bands vary at street scales, and are their statistical characteristics persistent over time and space?” Street-scale variations in the VHF and UHF bands exist and are significant, on the order of 20 to 30 dB depending on frequency and neighborhood. Characteristic noise cluster lengths, similarly dependent upon frequency and neighborhood, are generally on the order of 20 to 100 m. We also found that the impulsive content varies with urban areal density, with thermalized noise more likely observed in open areas. In terms of temporal persistence, median power displayed excellent repeatability, while peak power and voltage deviation showed a slightly lower repeatability, as expected due to their sensitivity to impulsive content. Overall, we found the spatial patterns of RF noise to be persistent features of the urban environment on timescales of hours to weeks and possibly beyond.

Given the large spatial variability in noise observed on the neighborhood scale, we note that the recent trend in the literature of using fixed position measurements to characterize entire environmental categories is not without risk. Noise mapping through spatially dense fixed measurements or the mobile noise measurement techniques as discussed here and in Spaulding et al. (1971) and appendix A of Spaulding and Disney (1974) can avoid this issue. A spatial understanding of the RF noise field can provide important and objective context for urban noise measurements, beyond that of choosing a measurement site based on its visual appearance, urban density, or accessibility.

Contrary to Spaulding et al. (1971), Spaulding and Disney (1974), Lauber and Bertrand (1999), and a host of other earlier works on urban RF noise, our measurements indicate that vehicular traffic density appears to be unimportant for predicting any of our summarizing statistics, in either neighborhood. For example, vehicular traffic in Downtown (MassDOT, 2010) is heaviest (15,000 to 30,000 vehicles per day) along Atlantic Ave. on the southeastern edge of the neighborhood and lighter (generally <5,000 vehicles per day) within the core. It is surprising then that our lowest values for median and peak power in the entire neighborhood were recorded along Atlantic Ave. This finding, if it can be demonstrated in other cities, raises the question: Is modern urban noise at VHF and UHF dominated by building-related sources, rather than vehicular traffic as in decades past?

References

- Achatz, R. J. (1998). Man-made noise in the 136 to 138-MHz VHF meteorological satellite band (Technical Report TR-98-355): National Telecommunications and Information Administration.
- Achatz, R. J., & Dalke, R. A. (2001). Man-made noise power measurements at VHF and UHF frequencies (Tech. Rep. NTIA Report 02-390): U.S. Dept. Commerce.
- Bland, J., & Altman, A. (1987). Statistical methods for assessing agreement between measurement. *Biochimica Clinica*, 11, 399–404.
- Breton, D., & Haedrich, C. (2019). Urban radio frequency noise measurements at VHF and UHF from Boston, MA, October 2018. <https://doi.org/10.6084/m9.figshare.8186909.v1>
- Bruckert, E. J., & Sangster, J. H. (1969). The effects of fading and impulse noise on digital transmission over a land mobile radio channel, *20th IEEE, Vehicular Technology Conference* (vol. 20, pp. 14–17). <https://doi.org/10.1109/VTC.1969.1621959>
- Buehler, W. E., & Lunden, C. D. (1966). Signature of man-made high-frequency radio noise. *IEEE Transactions on Electromagnetic Compatibility, EMC-8*(3), 143–152.
- Crichlow, W., Roubique, C., Spaulding, A., & Beery, W. (1959). Determination of the amplitude-probability distribution of atmospheric radio noise from statistical moments. *Journal of Research of the National Bureau of Standards, 64D*(1), 49–56.

Acknowledgments

We would like to thank Jeffery A. Wepman of the Institute for Telecommunications Science for helpful discussions. The authors declare no financial conflicts of interest. Mention of specific equipment manufacturers does not imply endorsement or recommendation on behalf of the U.S. Government. Data supporting our conclusions (Breton & Haedrich, 2019) are archived at <https://doi.org/10.6084/m9.figshare.8186909.v1>. Additional maps and histograms of median power at 246.5 and 972 MHz can be found in the Supporting Information associated with this paper. This work was funded by the Assistant Secretary of the U.S. Army (Acquisition, Signature Physics and Terrain State Basic Research & Mapping and Remote Sensing) with portions funded under 611102T2400/T442/T24 and 61110252C00/T360/52C/01. Permission to publish was granted by Director, Cold Regions Research and Engineering Laboratory.

- Crichlow, W., Spaulding, A., Roubique, C., & Disney, R. (1960). Amplitude probability distributions for atmospheric radio noise, NBS Monograph 23, National Bureau of Standards.
- Cudak, M. C., Swenson, G. W., & Cochran, W. W. (1991). Airborne measurements of incidental radio noise from cities. *Radio Science*, 26(3), 773–781.
- Dalke, R., Achatz, R., Lo, Y., Papazian, P., & Hufford, G. (1997). Measurement and analysis of man-made noise in VHF and UHF bands. In *Proceedings of 1997 Wireless Communications Conference*, Boulder, CO, USA pp. 229–233. <https://doi.org/10.1109/WCC.1997.622284>
- Davenport, W., & Root, W. (1987). *An introduction to the theory of random signals and noise*, New York, NY, USA :IEEE Press.
- Esposito, R., & Buck, R. (1973). A mobile wide-band measurement system for urban man-made noise. *IEEE Transactions on Communications*, 21(11), 1224–1232.
- Fockens, T. W. H., Zwamborn, A. P. M., & Leferink, F. (2019). Measurement methodology and results of measurements of the man-made noise floor on HF in the Netherlands. *IEEE Transactions on Electromagnetic Compatibility*, 61(2), 337–343. <https://doi.org/10.1109/TEMC.2018.2830512>
- George, R. W. (1940). Field strength of motorcar ignition between 40 and 450 megacycles. *Proceedings of the IRE*, 28(9), 409–412. <https://doi.org/10.1109/JRPROC.1940.229381>
- Haedrich, C. E., & Breton, D. J. (2019). Measuring very high frequency and ultrahigh frequency radio noise in urban environments: A mobile measurement system for radio-frequency noise (Report ERDC/CRREL TR-19-8): Cold Regions Research and Engineering Laboratory (U.S.) <https://doi.org/10.21079/11681/33290>
- Keysight (2018). Noise figure measurement accuracy: The Y-factor method.
- Kozono, S., & Watanabe, K. (1977). Influence of environmental buildings on UHF land mobile radio propagation. *IEEE Transactions on Communications*, 25(10), 1133–1143. <https://doi.org/10.1109/TCOM.1977.1093736>
- Lauber, W. R., & Bertrand, J. M. (1999). Statistics of motor vehicle ignition noise at VHF/UHF. *IEEE Transactions on Electromagnetic Compatibility*, 41(3), 257–259.
- Leck, R. (2006). Results of ambient RF environment and noise floor measurements taken in the U.S. in 2004 and 2005(Tech. Rep. CBS/SG-RFC2005-5): World Meteorological Organization.
- Lee, Y. C., Achenbach, J. D., & Kim, J. O. (1993). Acoustic microscopy measurements to correlate surface wave velocity and surface roughness. In D. O. Thompson, & D. E. Chimenti (Eds.), *Review of Progress in Quantitative Nondestructive Evaluation* (Vol. 12, pp. 1791–1797). Boston, MA: Springer.
- MassDOT (2010). Traffic volume and classification.
- Middleton, D. (1973). Man-made noise in urban environments and transportation systems: Models and measurements. *IEEE Transactions on Communications*, 21(11), 1232–1241.
- Morse, M. D., & Patel, J. M. (2007). An efficient and accurate method for evaluating time series similarity. In *Proceedings of the 2007 ACM SIGMOD International Conference on Management of Data*, ACM, New York, NY, USA, pp. 569–580. <https://doi.org/10.1145/1247480.1247544>
- Palaios, A., Miteva, V. M., & Mahonen, P. (2018). Contemporary study of radio noise characteristics in diverse environments. *IEEE Access*, 6, 25,621–25,631. <https://doi.org/10.1109/ACCESS.2017.2654064>
- Parsons, J. D., & Sheikh, A. U. H. (1981). The magnitude of urban and suburban VHF man-made radio noise. *Radio and Electronic Engineer*, 51(11), 591–597.
- Paulson, A. (2019). Precision geolocation of propagation data using GPS and fusion. In *Proceedings of the 2019 IEEE International Symposium on Electromagnetic Compatibility, Signal & Power Integrity*, IEEE, New Orleans, LA.
- Ploussios, G. (1968). City noise and its effect upon airborne antenna noise temperatures at UHF. *IEEE Transactions on Aerospace and Electronic Systems*, AES-4(1), 41–51. <https://doi.org/10.1109/TAES.1968.5408932>
- Roy, T. N. (1981). Airborne man-made radio noise assessment (Tech. Rep. NOSC Technical Report 677): Naval Ocean Systems Center.
- SignalHound (2019). <https://signalhound.com/spike/>
- Skomal, E. N. (1965). Distribution and frequency dependence of unintentionally generated man-made VHF/UHF noise in metropolitan areas. Part II-Theory. *IEEE Transactions on Electromagnetic Compatibility*, 7(4), 420–427.
- Skomal, E. (1969). Analysis of airborne VHF/UHF incidental noise over metropolitan areas. *IEEE Transactions on Electromagnetic Compatibility*, EMC-11(2), 76–83.
- Skomal, E. N. (1970). The range and frequency dependence of VHF-UHF man-made radio noise in and above metropolitan areas. *IEEE Transactions on Vehicular Technology*, 19(2), 213–221.
- Skomal, E. (1975). Analysis of airborne VHF incidental noise over metropolitan areas—Part II: Horizontal dipole antenna. *IEEE Transactions on Electromagnetic Compatibility*, EMC-17, 77–84.
- Skomal, E. N. (1978). *Man-made radio noise*. New York: Van Nostrand Reinhold.
- Skomal, E. N., & Smith, A. A. (1985). *Measuring the radio frequency environment*. New York: Van Nostrand Reinhold.
- Spaulding, A. D., Ahlbeck, W. H., & Espeland, L. R. (1971). Urban residential man-made radio noise analysis and predictions (Tech. Rep. 14): Institute for Telecommunication Sciences.
- Spaulding, A. D., & Disney, R. T. (1974). Man-made radio noise, part 1: Estimates for business, residential, and rural areas (OT Report 74-38): U.S. Dept. Commerce, Office of Telecommunications.
- Wagstaff, A., & Merricks, N. (2005). Man-made noise measurement programme. *IEE Proceedings-Communications*, 152(3), 371–377.
- Wepman, J. A., & Sanders, G. A. (2011). Wideband man-made radio noise measurements in the VHF and low UHF bands (Tech. Rep. TR-11-478): National Telecommunications and Information Administration.

REPORT DOCUMENTATION PAGE

Form Approved
OMB No. 0704-0188

Public reporting burden for this collection of information is estimated to average 1 hour per response, including the time for reviewing instructions, searching existing data sources, gathering and maintaining the data needed, and completing and reviewing this collection of information. Send comments regarding this burden estimate or any other aspect of this collection of information, including suggestions for reducing this burden to Department of Defense, Washington Headquarters Services, Directorate for Information Operations and Reports (0704-0188), 1215 Jefferson Davis Highway, Suite 1204, Arlington, VA 22202-4302. Respondents should be aware that notwithstanding any other provision of law, no person shall be subject to any penalty for failing to comply with a collection of information if it does not display a currently valid OMB control number. PLEASE DO NOT RETURN YOUR FORM TO THE ABOVE ADDRESS.

1. REPORT DATE August 2020			2. REPORT TYPE Final		3. DATES COVERED (From - To)	
4. TITLE AND SUBTITLE Street-Scale Mapping of Urban Radio Frequency Noise at Very High Frequency and Ultra High Frequency					5a. CONTRACT NUMBER	
					5b. GRANT NUMBER	
					5c. PROGRAM ELEMENT NUMBER 0611102T	
6. AUTHOR(S) Daniel J. Breton, Caitlin E. Haedrich , Matthew J. Kamrath, and D. Keith Wilson					5d. PROJECT NUMBER T442	
					5e. TASK NUMBER 01	
					5f. WORK UNIT NUMBER	
7. PERFORMING ORGANIZATION NAME(S) AND ADDRESS(ES) U.S. Army Engineer Research and Development Center Cold Regions Research and Engineering Laboratory 72 Lyme Road Hanover, NH 03712					8. PERFORMING ORGANIZATION REPORT NUMBER ERDC/CRREL MP-20-10	
					9. SPONSORING / MONITORING AGENCY NAME(S) AND ADDRESS(ES) U.S. Army Corps of Engineers Washington, DC 20314-1000	
10. SPONSOR/MONITOR'S ACRONYM(S) USACE					11. SPONSOR/MONITOR'S REPORT NUMBER(S)	
					12. DISTRIBUTION / AVAILABILITY STATEMENT Approved for public release; distribution is unlimited.	
13. SUPPLEMENTARY NOTES Originally published in Radio Science, 18 December 2019. This work was funded by the Assistant Secretary of the Army (Acquisition, Signature Physics and Terrain State Basic Research & Mapping and Remote Sensing) with portions funded under 611102T2400/T442/T24, 61110252C00/T360/52C/01.						
14. ABSTRACT Modern measurement campaigns of man-made radio frequency (RF) noise have reported results from fixed locations that are assumed to be representative of the surroundings. Models derived from these measurements include parameters to express the variability in time and in space over very large distances (i.e., differences between cities). Despite the rapidly evolving mixture of noise sources, especially in modern urban environments, spatial variation of RF noise power at the scale of streets and blocks essentially unknown in the very high frequency and ultra high frequency bands. Using a portable calibrated noise measurement system of our design, RF noise was recorded over a 1-MHz bandwidth for frequencies of 142.0, 246.5, and 972 MHz. Noise surveys were conducted during daytime working hours in two different neighborhoods within Boston, Massachusetts, USA, with each survey transiting a fixed, several kilometer long route, repeated twice to enable separation of temporal from spatial variability. Significant and spatially repeatable variations in median power, peak power, and voltage deviation were observed over distances of tens to hundreds of meters, dependent upon the measurement frequency. The observed spatial patterns of median and peak power appear to be repeatable on timescales of hours to weeks, and likely beyond, suggesting that these noise patterns are persistent features of the urban environment.						
15. SUBJECT TERMS Urban, Radio frequency, Noise, Geospatial, Impulse						
16. SECURITY CLASSIFICATION OF:				17. LIMITATION OF ABSTRACT	18. NUMBER OF PAGES	19a. NAME OF RESPONSIBLE PERSON
a. REPORT Unclassified	b. ABSTRACT Unclassified	c. THIS PAGE Unclassified		UU	18	19b. TELEPHONE NUMBER (include area code)